ABSTRACT

Title of thesis : Design of a Real Time Optical Sensor for continuous Blood Cell Separation.

Girish S. Yerande, Master of Science in Electrical Engineering, 1990.

Thesis Directed by: Dr. Sam S. Sofer, Professor,

Sponsored Chair in Biotechnology.

For continuous measurement and display of oxygen saturation and RBC content in blood during cell separation a reflection type optical sensor is designed based on the theoretical model using the photon diffusion theory. The prototype sensor consists of two arrays of light emitting diodes, red and infrared, and photodiodes. The emission wavelength of LEDs are 660 nm and 800 nm. The 800 nm which is in the infrared region is very close to isobestic value for blood. The prototype sensor is mounted on the blood cell separator equipped with an antitwister mechanism. Each LED emits a specific wavelength of light through the blood chamber to the photodiode. Since oxygen saturated blood absorbs differing amounts of light at each wavelength as compared to unsaturated blood, the amount of light absorbed by the blood in each pulse can be used to calculate the oxygenated hemoglobin to total hemoglobin.

The conventional reflection type dual wavelength method is modified adding the constants C_1 and C_2 as $(R660 + C_1)/(R800 + C_2)$, where R660 and R800 are the reflectances at 660 and 800 nm, and C_1 and C_2 depend upon the sensor geometry and the blood physiological characteristics. These constants are calculated using blood

physiology, hematocrit variations, the sensor model and the cell separator model. Changes in the constants are corrected by a microprocessor for online sensor adjustments.

The oxygen saturation and RBC content are displayed on the LED displays and are updated once a second. The sensor position on the blood chamber is indicated visibly by a LED array. The audio alert indicates the lower RBC content. The scattering of light at the boundary of red blood cells and white blood cells is sensed to control the electromechanical valve and the sampler. This valve and the sampler are used to collect the samples for further blood analysis. The microprocessor is used for controlling the system, storage of the signal level and comparison of signal ratios.

The long-term aim is to design a reliable, intelligent, real time, online sensor system for blood cell separation devices.

DESIGN OF A REAL TIME OPTICAL SENSOR FOR CONTINUOUS BLOOD CELL SEPARATION.

by

Girish S. Yerande

Thesis submitted to the Faculty of the Graduate school of
the New Jersey Institute of Technology in partial fulfillment of
the requirements of the degree of
Master of Science in Electrical Engineering.
1990

APPROVAL SHEET

Title of Thesis : A Real Time Optical Sensor for Continuous Blood Cell Separation.

Name of Candidate : Girish Yerande
Master of Science in
Electrical Engineering, 1990.

Thesis and Abstract Approved by : ---------- 9/13/90

Dr. Sam Sofer, Professor, Date
Sponsored Chair in Biotechnology.

---------- 9-13-90

Dr. William Carr, Professor, Date
Sponsored Chair in Microelectronics.

Signatures of other members of the thesis committee

---------- 9-13-1990

Dr. Edip Niver, Professor, Date
Dept. of Elect. Engg.

VITA

Name: Girish S. Yerande

Permanent Address: 178 Union Avenue, 2nd floor, Belleville, NJ 07109.

Degree and Date to be conferred: M.S.E.E., 1991.

Secondary Education: Chaitanya Vidyalaya, Poona, India.

Collegiate Institutions Attended	Dates	Degree	Date of Degree
New Jersey Institute of Technology, Newark, NJ	Sep 88 to Aug 90	M.S.E.E.	Oct 1991
SGGS College of Engg. and Technology, Maharashtra, India.	Aug 83 to Jun 86	B.E.	Jul 1986
Government Polytechnic, Poona, India.	Aug 80 to Jul 83	Diploma	Jul 1983

Major: Electrical Engineering.

Publication : "Design of a real time optical sensor for continuous blood cell separation." to be submitted to Biosensors.

ACKNOWLEDGEMENT

I would like to express my sincere gratitude to my supervising advisor Dr. Sam S. Sofer for his keen, creative and invaluable guidance, friendship and moral support throughout this research. Without his chemical expertise and jovial manner, the design aspects of this project would not have been accomplished. I am thankful to him for helping me to be a design oriented electrical engineer as I always desired.

I am grateful to Dr. Niver and Dr. Carr for being on the panel of advisors and for their able guidance on the optoelectronic aspect of the project. Dr. Niver's course on integrated and fiber optics and his timely help for the design was of immense help.

I am thankful to my friends Tim, Ajit and Anju for their help in blood separation techniques and design clues.

I am thankful to Vivek, Amos and all other members of the biotechnology lab for their cooperation.

I am thankful to Emilia and Fayaz for their timely help at every stage.

I have special regards for Sandeep, Ravi, Nitin, Ashfaque, Abhay and Sanjay for their contribution to work that meant lot to me.

Finally, I do not have the words to express my gratitude to my parents, elder brother Shree and family members. Their graciousness, understanding and motivation played a major role in achieving my goal.

And most of all thanks to the Almighty Lord.

Contents

List of Figures

Chapter 1

Introduction

The levels of pO_2, pCO_2, and pH in the blood are the fundamental measures in the diagnosis and treatment of pulmonary disorders. Measurement of the oxygenation of blood at different sites in the circulatory system can provide valuable information about the condition of the heart and lungs, the adequacy of perfusion of other vital organs and the presence of metabolic abnormalities. In some of the physical and clinical monitoring applications in which intermittent sampling has been used to assess blood oxygenation, a reliable, real time sensor is required. For example, continuous oxygen monitoring is needed in the management of cardiac surgery patients, neonatal and fetal research and the study of organ level oxygen transport during circulatory shock.

We, at NJIT Biotechnology Laboratory, are doing research in four different areas, led by the Detox group, Blood group, Bioproducts group and Food processing group. All these fields depend on accurate sensing of oxygen. For example, the Detox group requires oxygen sensors for the study of reaction rates for decontamination of water,

the blood group to detect the oxygen level in the patient blood, the food technology group for the study of viability of yeast and the bioproducts group to monitor liver enzyme reactions.

Presently the blood processing group is involved in developing an extracorporeal detoxifier to remove diseased white cells, which has a potential application in treatment of AIDS and cancer. The experimental extracorporeal device is a centrifugal cell separator, which can be used to collect different blood components. This requires the real time online sensing of oxygen as well as RBCs in separating blood.

In view of this need an optical sensor is designed using the photon diffusion theory. The general concept and the design aspect of this sensor was provided by Dr. Sam S. Sofer. The sensor arrays are mounted on the blood cell chamber of the cell separator. The separator is equipped with an antitwister mechanism. The oxygen saturation and the RBC content in the separating blood are to be measured. The sensor system will be developed further with a fiber optic probe for the other applications such as whole blood and chemical reactions.

The earlier innovation by Brinkman *et al* [1] in 1949 yielded an instrument called 'Cyclops' by which reflection from the forehead was analyzed for obtaining arterial hemoglobin Oxygen Saturation (OS) noninvasively. In 1962, Polanyi and Hehir [2] established the basis of modern reflection oximetry. They used fiber optics to guide the light at a specific wavelength into the blood stream and to measure the hemoglobin OS *in vivo*. In 1972, Johnson *et al* [3] devised a fiber optic oximeter, and the catheter tip hybrid type system was later developed by Yee *et al* [4].

For deriving hemoglobin OS, the optical reflection measurement in whole blood, an empirical method derived by Polanyi and Hehir [2] computed the ratio of reflectances at two specific wavelengths, one in the red region and other in the near infrared region, and approximated hemoglobin OS using the following relation ,

$OS = A + B + R_{805}/R_{665}$,

Where R_{805} and R_{665} are the reflectances at the wavelengths of 805 and 665 nm, and A and B are the constants that depend on the characteristics of blood and sensor. However, due to the nonlinear effect of light scattering at the interface of plasma and red blood cells (RBCs) this method may yield some error unless the correction is made as the hematocrit variations occur. Also the nonlinear relation between the reflection ratio and hemoglobin OS at the lower OS values may add some errors when this method is used for venous blood. In order to overcome this error, Pittman and Duling added a third wavelength at the isobestic region (where the absorption is independent of Oxygen Saturation) in the transmission measurement [5]. A different approach was taken by Lubbers *et al* who employed a multicomponent analysis to deal with the nonlinear effect of scattering [8].

In 1988, Setsuo Takatani *et al* [18] added a constant term C in the denominator as R_{795} / R_{665}+C, where R_{795} and R_{665} are the reflectances at 795 and 665 nm and C depends on the sensor geometry and the blood physiological characteristics. The prototype sensor was tested in human, calf and goat whole blood over the hematocrit range of 20 - 45 percent.

Here we utilize the sensor arrays that consist of light emitting diodes (LEDs) and photodiodes. Each LED emits a specific wavelength of light (660 nm and 800 nm),

through the blood separating in the blood cell chamber of the cell separator to the photodiode. Oxygen saturated whole blood absorbs differing amounts of light at each wavelength compared to unsaturated blood. The same principle was applied to the separating blood. The LEDs emitted light alternately with the fixed frequency.

The LEDs and photodiodes are mounted above and below the cell separating chamber. The amount of light absorbed by the blood is used to calculate the ratio of oxygenated hemoglobin to total hemoglobin. This is displayed as OS. The continuous monitoring of the separating blood is achieved without collecting the blood samples. The error is reduced by introducing the constants C_1 and C_2 as $(R660 + C_1)/(R800 + C_2)$, where $R660$ and $R800$ are the reflectances at 660 nm and 800 nm and C_1 and C_2 are the constants which depend upon the sensor geometry, hematocrit variations and blood physiology.

Our approach was towards the instrumentation for sensing and control of the overall blood separation process, such as sensing of oxygen saturation and RBC content, opening and closing of valves and control of a sampler for blood sample collection, and audio alerts for low RBC content. The output is in real time and digital form.

Chapter 2

Theoretical Background

2.1 Optical Diffusion in Blood

Kramer performed experiments with whole ox blood [15], and measured transmittance at several wavelengths versus blood layer thickness and oxygen saturation and showed that transmittance did not obey the simple exponential law (Beer's law):

$I = I_0 e^{-\alpha d}$,

where

I = transmitted intensity,

I_0 = incident intensity,

α = loss factor, and

d = blood layer thickness.

The loss was much greater than expected from experiments with hemolyzed blood, and did not vary exponentially with d. Anderson and Sekelj [19][20] measured transmittance and reflectance of fully oxygenated red cells. Their measurements were for thin slabs of blood in the wavelength range of $\lambda = 0.50$ to $\lambda = 0.63$ microns. Hemat-

ocrit, defined as the ratio of the volume of red cells to total blood volume was varied over a wide range. These results showed that transmittance did not obey Beer's law, but was described by Twersky's multiple scattering theory. Transmittance of rabbit's blood at $\lambda = 0.805$ micron was measured versus blood layer thickness and hematocrit by Loewinger *et al* [21]. Their results were similar to those of Kramer and Anderson and Sekelj. They noted that density OD defined as $OD = log_{10} I_0/I$, is nearly linear versus blood layer thickness for large hematocrit values. Johnson [9] measured relative transmittance versus d. The experimental plots are shown in Fig.(2.1). The distance between the scatterers (blood components) increases as hematocrit decreases and thus the diffusion penetration depth increases.

2.2 Application of photon diffusion theory

For optical propagation in blood, for oximetry, various theories such as the multiple scattering theory, the two flux theory, and the photon diffusion theory are tried. If the medium satisfies the assumption underlying the diffusion theory, photon diffusion theory can yield an accurate solution [5]. For separating blood this theory is applied. This theory can be used to design the sensor geometry as the solution can be expressed in a three dimensional model. For whole blood, Johnson *et al* [9] demonstrated that above the 5-10 percent hematocrit range optical diffusion takes place in whole blood, and derived a differential equation governing the scattered photon density in cylindrical coordinates. It is stated as

$$(\nabla^2 - f_a/D)\rho_s(r, \theta, z) = -(f_s/D)S_o,$$

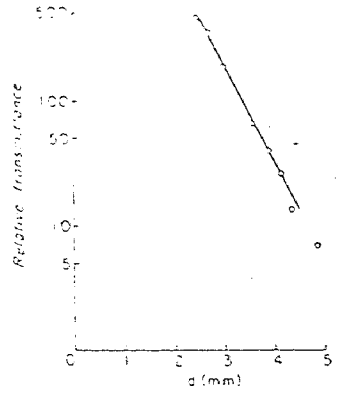

(a)

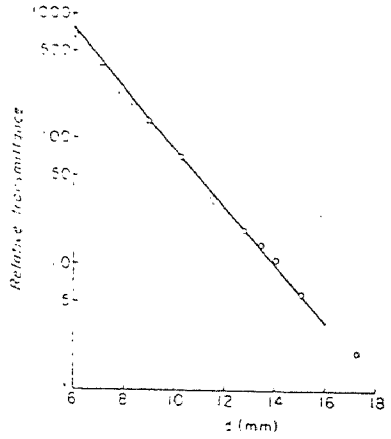

(b)

Figure 2.1: Relative transmittance versus d (a) for HCT = 0.08 (b) for HCT = 0.40 (Source : [9])

where ρ_s is the scattered photon density in cylindrical coordinates, f_a and f_s are the diffusion absorption and scattering constants of the medium respectively and D is its diffusion constant given by $\nu^2/(2f_s + f_a)$ with ν being the velocity of light. The source function S_o can be expressed in terms of isotropic or anisotropic scatterers, depending entirely upon the optical characteristics of the medium.

The solution to this equation for a two layer tissue model with each layer being homogeneous and isotropically scattered was obtained by Takatani and Graham [10] and it was applied to the reflection oximetry of gut mucosa. The two layer solution can be simplified if the single layer can satisfy an assumption of the semi-infinite extent that underlies the photon diffusion theory, as obtained by Reynolds [11] which was used by Takatani *et al*[18] :

$$R(r_a) = \left[\frac{2}{d}\right]\left[\frac{S}{S+K}\right]\left[\sum_{n=1}^{\infty} A_n[1 - e^{-d/\delta_0}(-1)^n]\right] \times \left[1 - \frac{2r_a}{b} M_1(\gamma_n b) N_1(\gamma_n r_a)\right] \quad (2.1)$$

where $R(r_a)$ = all the reflected light collected within the circle of radius r_a at the $z = 0$ plane.

S, K = scattering and absorption constants of the medium.

d = thickness of the medium.

b = radius of the light source.

δ_0 = penetration depth of the incident photon given by 1/(S+K).

γ_n = eigenvalues given by $[(1/\delta_d)^2 + (n\pi/d)^2]^{1/2}$.

M_1, N_1 = first order Bessel's function of the first and second kind, respectively.

$$A_n = \frac{\delta_0}{1 + (\delta_0/\delta_d)^2 + (n\pi\delta_0/d)^2 + (d/n\pi\delta_d)^2}. \quad (2.2)$$

δ_d = diffusion length defined as $[K(2S + K)]^{1/2}$.

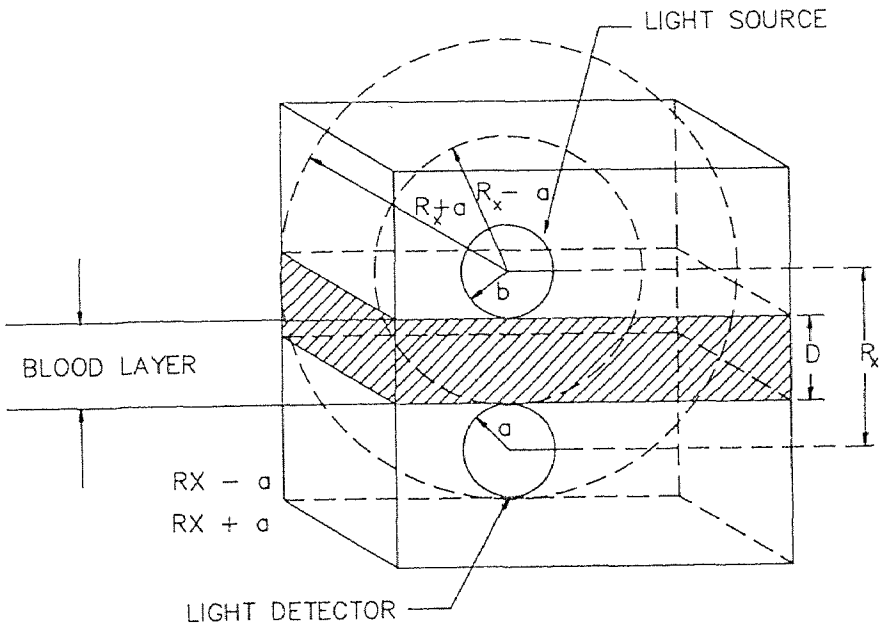

Figure 2.2: Sensor Model for computation of diffuse reflectance

.3 Mathematical Modelling

. this study the isotropic diffusion equation [2.1] [18] in combination with the sensor odel as shown in Fig. (2.2), was used to derive the diffuse reflectance from the parating blood. Referring to Fig. (2.2), in computation of the diffuse reflectance R_d ceived by the photodetector with its aperture radius of a, first the diffuse reflectances ithin circles of radius $r_1 = R_x - a$ and $r_2 = R_x + a$, denoted here as $R(r_1)$ and $R(r_2)$ e computed using equation [2.1]. Then the diffuse reflectance R_d is the difference $R(r_1)$ and $R(r_2)$ weighted by the area ratio factor of $a_2/(r_2^2 - r_1^2)$ and given as

$$R_d = [a^2/(r_2^2 - r_1^2)][R(r_2 - R(r_1)]. \tag{2.3}$$

he absorption and scattering constants of the medium, K and S, were expressed in rms of hematocrit (H), hemoglobin OS, scattering and absorption cross section of ıe RBCs and RBC density by the following equations [10] :

$$S = \sigma_S^- \times (1 - H) \times \rho, and \tag{2.4}$$

$$K = \rho \times [\sigma_{a0} \times OS + \sigma_{ar} \times (1 - OS)]. \tag{2.5}$$

In equations (2.4) and (2.5), σ_s is the backscattering cross section of the single BC, $\sigma_a 0$ and $\sigma_a r$ are the absorption cross sections of the oxygenated and deoxy- enated RBCs, respectively, and ρ is the density of RBCs given by H/V where V is ıe mean RBC volume. The value of σ_s^- is approximately constant in the red and ıfrared regions. The experimentally determined value is $0.558\mu^2$ [23]. The values of oth σ_{a0} and σ_{ar} are wavelength dependent[10].

2.4 Optical Sensor

1) Source-Detector separation distance and wavelength selection:

The distance that the incident photons penetrate into the medium before they are diffused is called the incident photon penetration depth and is defined as 1/(S+ K) [7]. Within this region, the direction of propagation is governed by the incident direction and usually multiple scattering occurs. If the detector is placed close to the light source within the multiple scattering region, the measurement includes the effects due to surface scattering and multiple scattering that occurs within the region of penetration depth. Therefore, based on diffusion analysis, source detector separation distance should be made larger than the penetration depth, to ensure that the detector captures mainly the diffused light. This will eliminate effects such as scattering at the surface and in the boundary region and will allow the detection of diffused light returning from the deeper layer of the medium.

Fig. (2.3 a) shows the penetration depths into the whole blood as a function of hemoglobin OS and wavelengths as obtained from equations (2.4) and (2.5). The penetration depth is a function of wavelength because both the scattering and absorption of light are wavelength dependent. For a wavelength shorter than 600 nm, absorption by hemoglobin is so strong that the photons cannot penetrate into the whole blood more than 0.1 mm, while at a wavelength longer than 600 nm, optical absorption decreases, and for the hematocrit value of 45 percent the penetration depth of the incident photons into whole blood is around 0.3 - 0.5 mm. Thus, it is advised that in order to avoid the effects of multiple scattering, the source detector distance should be made larger than the penetration depth, at least 2 -3 mm.

$$\delta_0 = 1/(S + K)$$

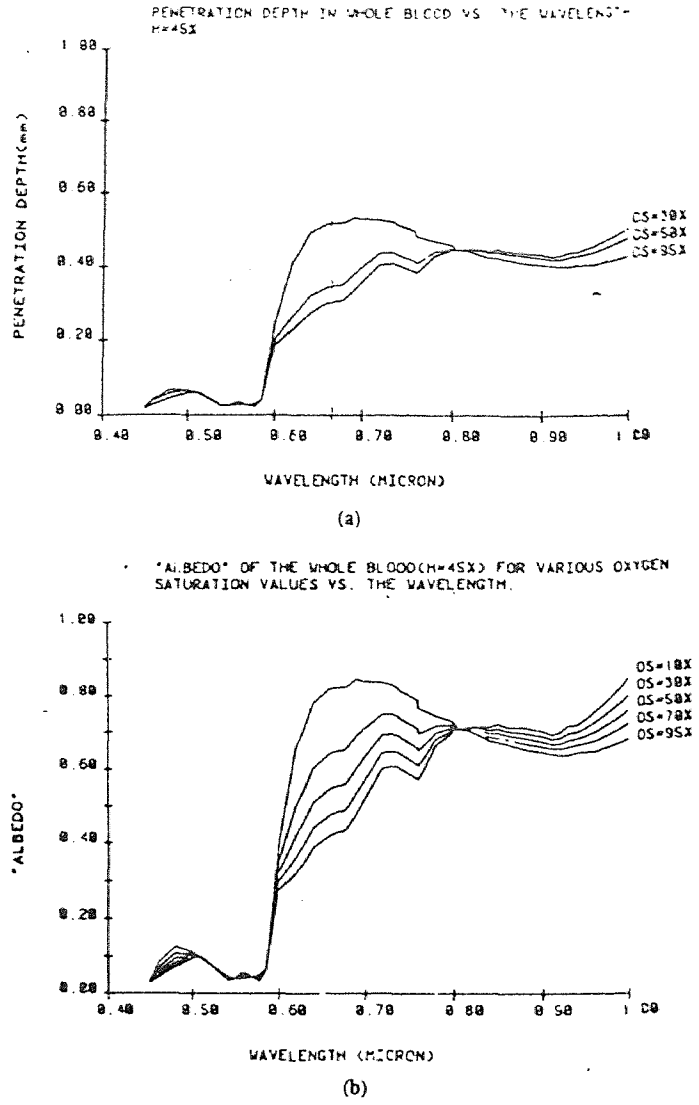

Figure 2.3: Penetration Depth (a) and albedo (reflectance)(b) of whole blood versus wavelength. (Source : [18])

Chapter 3

Sensor System Design

3.1 Design Setup

The block schematic of the oximeter system design is shown in Fig.(3.1). The sensor head consists of arrays of 5 red and 5 infrared LEDs placed above the blood cell chamber and an array of 5 photodiodes placed below the blood cell chamber. The sensor head is mounted inside the blood cell separator. The light is passed through the blood layer with the known frequency which is generated by the timing generator from the sensor board assembly. The diffused light through the blood is detected by the photodiodes. Only one LED flashes at a time which avoids the cross light interference.The analog signal is retrieved. The front panel controls are used for display and control of the overall blood separation process.

The sensor board may be interfaced to the personal computer with a machine such as the K-8073 processor. Also the electromechanical valve and the sampler are controlled by the relays which are controlled by the sensor board. This valve and the sampler are used to collect the blood samples for the blood cell analysis.

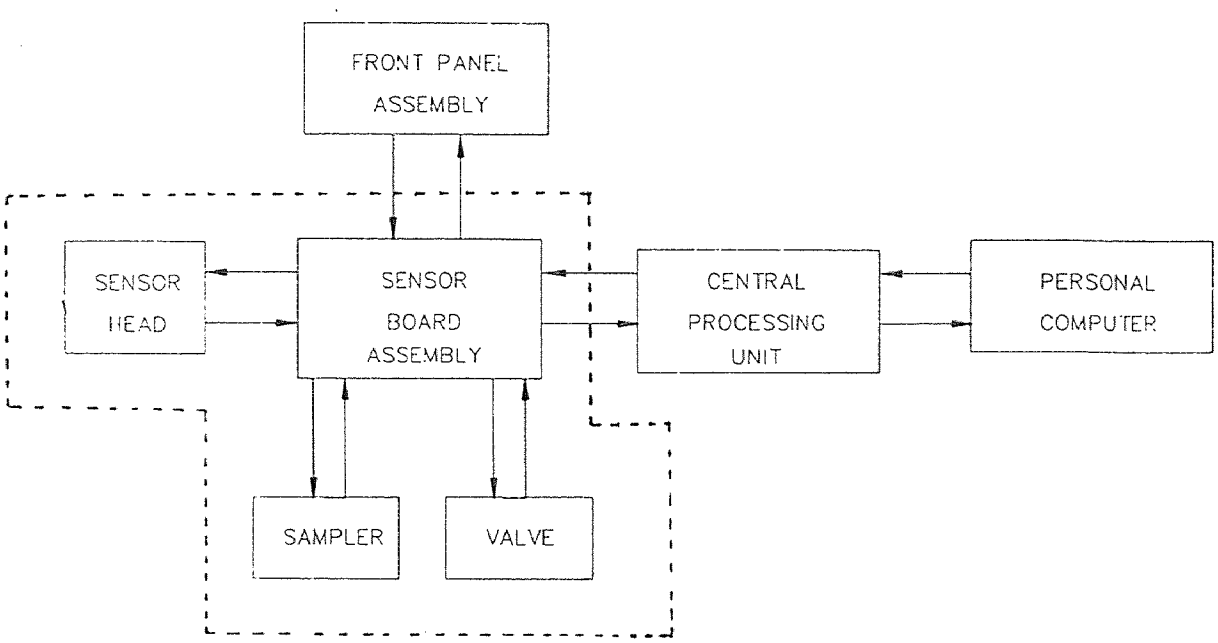

Figure 3.1: Block Schematic of the Sensor System.1) OS and RBC content 2)Remaining Portions Proposed.

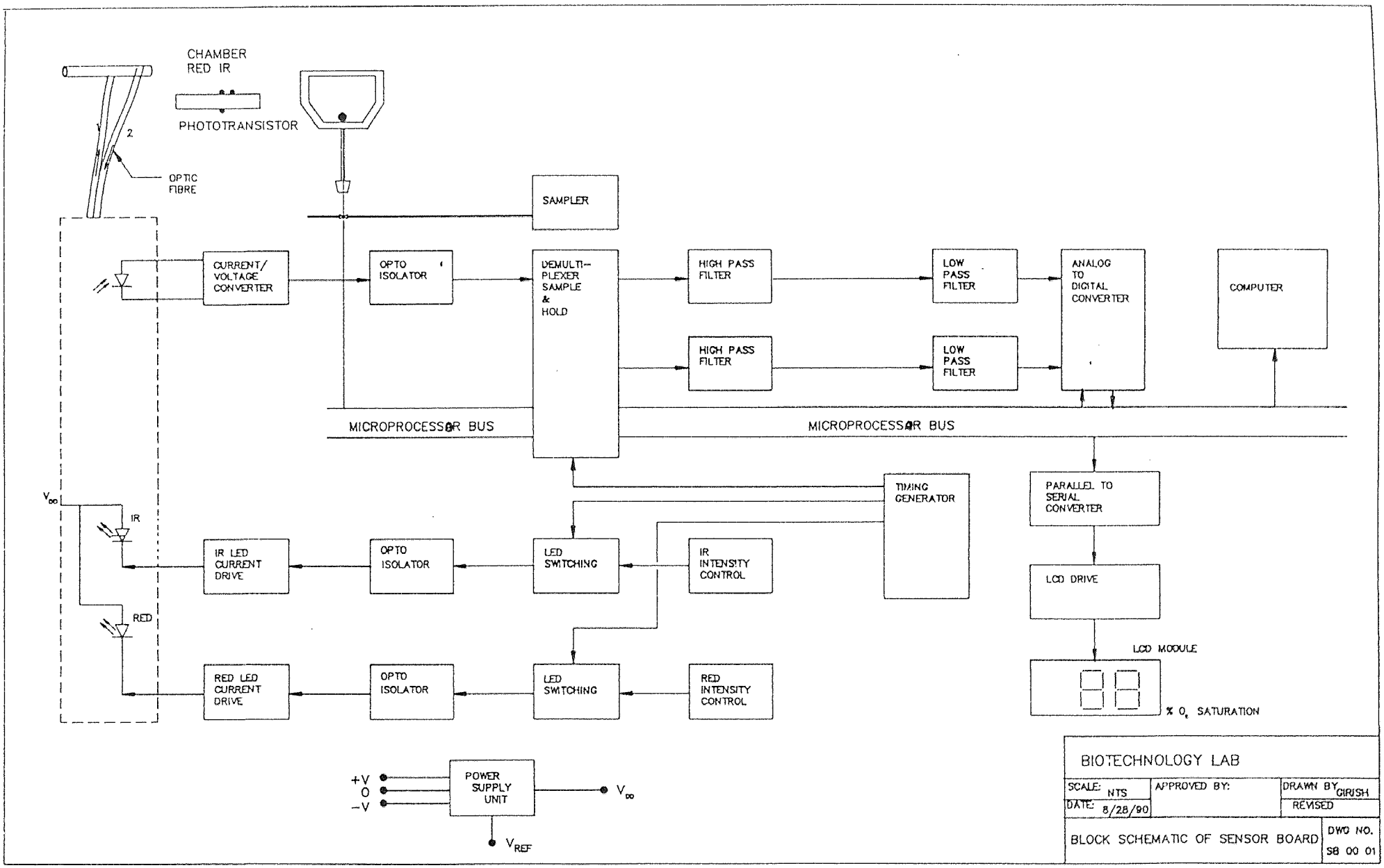
CHAMBER
RED IR
PHOTOTRANSISTOR
OPTIC FIBRE
SAMPLER
CURRENT/ VOLTAGE CONVERTER
OPTO ISOLATOR
DEMULTI-PLEXER SAMPLE & HOLD
HIGH PASS FILTER
LOW PASS FILTER
HIGH PASS FILTER
LOW PASS FILTER
ANALOG TO DIGITAL CONVERTER
COMPUTER
MICROPROCESSOR BUS
MICROPROCESSOR BUS
TIMING GENERATOR
PARALLEL TO SERIAL CONVERTER
IR
RED
IR LED CURRENT DRIVE
OPTO ISOLATOR
LED SWITCHING
IR INTENSITY CONTROL
LCD DRIVE
LCD MODULE
RED LED CURRENT DRIVE
OPTO ISOLATOR
LED SWITCHING
RED INTENSITY CONTROL
% O_2 SATURATION
+V
0
-V
POWER SUPPLY UNIT
V_{DD}
V_{REF}
BIOTECHNOLOGY LAB
SCALE: NTS
APPROVED BY:
DRAWN BY GIRISH
DATE: 8/28/90
REVISED
BLOCK SCHEMATIC OF SENSOR BOARD
DWG NO. SB 00 01

The design of the sensor board assembly is explained in detail as follows.

3.2 Design of Sensor Board Assembly

The block schematic of the sensor board assembly is shown in Fig.(3.2). The operational functions of the sensor board assembly can be broken down as follows:

1. Power Supply Unit,
2. Red and Infrared LED Drive,
3. Timing Generator,
4. Signal Retrieval,
5. Analog to Digital Conversion, and
6. Control Signals.

The circuit diagram of the sensor board assembly is shown in Fig.(3.3)

3.2.1 Power Supply Unit

The line transformer T1, steps the line voltage (110V AC) down to 9V rms. The stepped down voltage is full wave rectified by D1. The rectified output is filtered by C1 and C2. The +5V regulator IC1 supplies power to the system. The 6.2V zener diode D2 protects the circuits from an overvoltage situation in the event of an IC1 failure.

The +V supply is derived from VDD supply on the CPU board. IC2 takes the +5V supply and creates a -VA supply (-5V) which is complimented to +VA supply (+5V).

Figure 3.3: Circuit Diagram of Sensor Board Assembly.(see pocket)

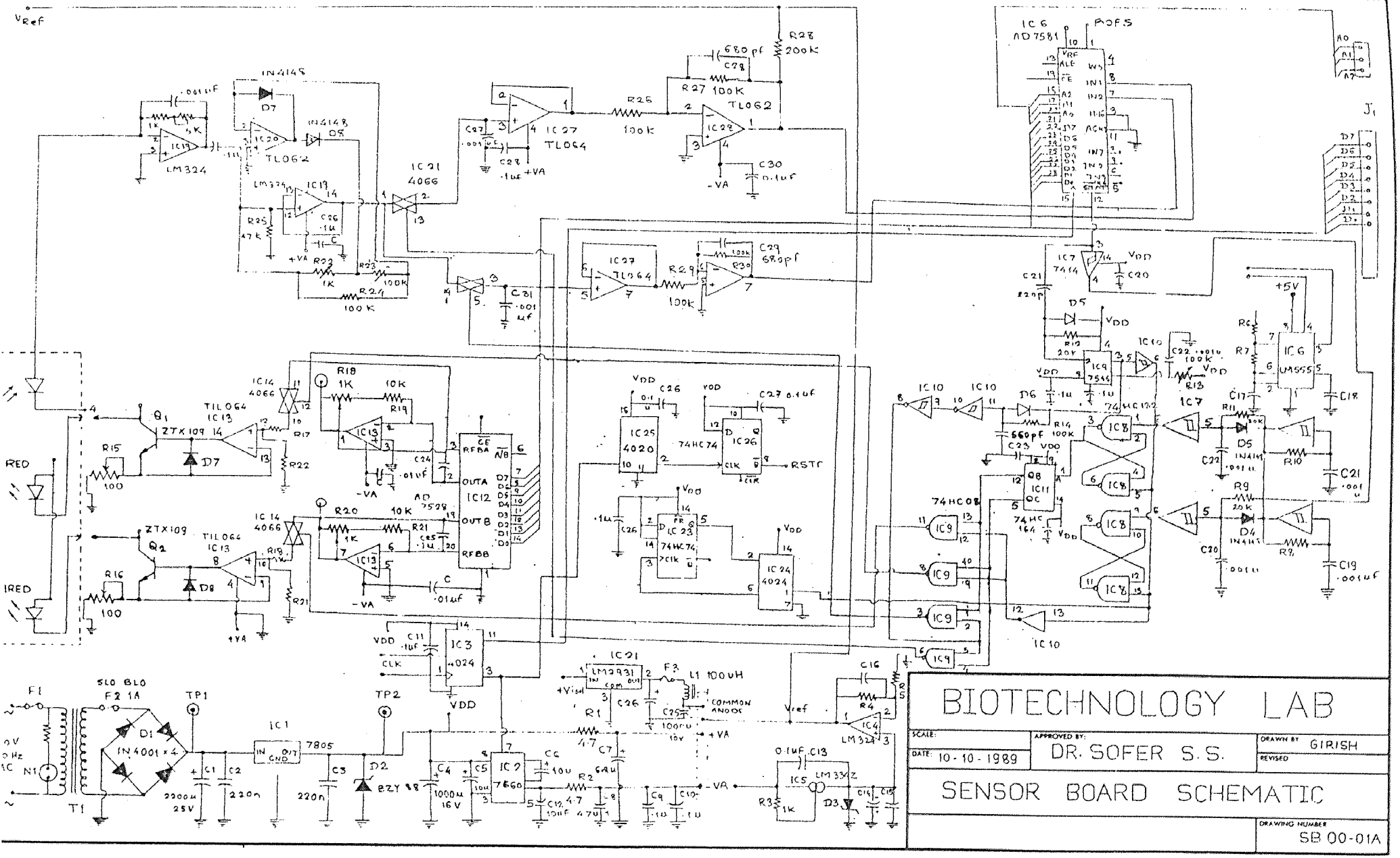
BIOTECHNOLOGY LAB
SCALE:
DATE: 10-10-1989
APPROVED BY: DR. SOFER S.S.
DRAWN BY: GIRISH
REVISED
SENSOR BOARD SCHEMATIC
DRAWING NUMBER: SB 00-01A

Table 3.1 : Component specifications of the sensor board assembly circuit.

Part No.	Description
T1	Tranformer 110V/9Vrms, 60Hz
N1	Neon Lamp
D1	Bridge Rectifier, 1N4001
F1, F2	Fuse 1A, slo blo
C1	Capacitor 2200 μf, 25V, Elect. radial
C2, C3	Capacitor 220 nf, multilayer ceramic
IC1	IC 7805, +5V regulator
D2	Diode zener 6V2 5 % 500 mW
IC2	ICL7660CPA
C4	Capacitor 100 μf, 25V
C5, C6, C12	Capacitor 10 μf, 25V
C7	Capacitor 6.8 μf, 25V
R1, R2	Resistor 4.7 ohm 1/4 W
C8	Capacitor 4.7 μf, electrolytic
C9, C10	Capacitor 0.1 μf, disc
C11, C12	
C15	
IC3	CD4024BE, 7 stage binary counter
IC4	LM324Z Quad. op. amp
IC5	LM334Z Constant current source
IC6	AD7581JN 8 bit analog to digital converter
IC7	MM74HC14N
IC9	M7555IPA
IC10	MM74HC14N
IC11	74HC164 8 bit shift register
IC12	AD7528 dual digital to analog converter
R3	Resistor 1k,1/4W, 10%
C16	Capacitor 0.1 μf, 500V, poly.
R4	Resistor 13k, 1/4W, 10%
R5	Resistor 12.7k, 1/4W, 10%

Part No.	Description
D3, D4	Diodes 1N4148
R13, R14	Resistor 100 k variable
R15, R16	Resistor 100 ohms, 1/4W, 10%
IC13	Op. amp. TLO64TN
R17, R18	Resistor 200 K, 1/4W, 10%
R18, R20	Resistor 1K,1/4W, 10%
IC14	CD4026
C21	Capacitor 220 pf
C23	Capacitor 560 pf
L1	Choke 100 μH
C25	Capacitor 1000 μf
IC21	LM 2931
F3	Fuse 1/10 A Fast Blo
IC23	74HC74
C26, C27	Capacitor 0.1 μf
IC25	CD4020
IC26	74HC74
D7, D8	Diode 1N4148
R22	Resistor 1K variable
R23	Resistor 100 K variable
R24	Resistor 100 K, 1/4W, 10%
R25	Resistor 47 K,1/4W, 10%
C27	Capacitor .001 μf
IC27	Op. amp. TL064
IC28	Op. amp. TL064
R26	Resistor 100 K, 1/4W, 10%
C28	Capacitor 680 pf
R27	Resistor 100 K, 1/4W, 10%
R28	Resistor 200 K, 1/4W, 10%
R29	Resistor 100 K, 1/4W, 10%
R30	Resistor 100 K, 1/4W, 10%
C29	Capacitor 680 pf
IC5	Timer NE555.

The switching frequency is set and phase locked into the system clock by the 7 stage binary counter IC3/3 (CD4024BE). Decoupling from any high frequency is provided by R2 and C8 for negative supply and by R1 and C7 for positive supply.

3.2.2 2.5 V Reference Supply

An 2.5V reference supply V_{ref} is developed at IC4/1(LM324). which is derived from zener diode D3. D3 is biased by the constant current source IC5 (LM334Z) and R3.

3.2.3 Sensor LED Supply

The +Visol supply is regulated by IC21, LM2931. Noise produced by the switching of the sensor LED is decoupled by L1 and C25. The fuse F3 protects the sensor from any damage if any part of the LED drive fails.

3.2.4 RSTC Interrupt

The RSTC interrupt is generated when IC26/8 goes low. The 4 MHz system clock is divided down by IC3 and IC25 to 4 MHz at IC7/2. The positive going edge of the pulse at IC26/11 sets IC26/8 low and an interrupt is requested. The output at IC26/8 is reset to a high when the software reads addresses. The RSTC is used in applications such as updating displays, sampler rotation, opening and closing of valve.

3.2.5 Red and Infrared LED Drives

The red and infrared LED drive channels operate identically. The red channel is explained below. The corresponding infrared devices are shown in brackets[ ].

The LED drive current is controlled by the dual digital to analog converter IC AD7528, IC12. The DAC is set by the software to control the output voltage of the buffer IC12/7. IC12/1 [IC12/7] can be set to any DC voltage within the range of 0 VA to -Vref at the converter output and then inverted by the op amp. The output of IC12/1 [IC12/7] is fed into an analog switch IC14/11 [IC14/8]. The switch is controlled by the timing generator output at IC9/8 [IC9/11]. The switch output at IC14/10 [IC14/9] is a pulse with an amplitude matching the DC level at switch input.

The switch output is attenuated by R17, R22 [R18, R21] and drives the buffer at IC13/14 [IC13/8]. The buffer sets the base voltage for the transistor Q1 [Q2], an emitter follower. The collector of the transistor drives the optocoupler LED IC16 [IC17]. The optoLED current and therefore LED light intensity is directly proportional to voltage pulse. The IC1814 [IC18/8] output drives the buffer IC 18/1 [IC18/7] which sets the base voltage of the emitter follower . The resulting pulse across the resistor sets the collector current and so the sensor LED current.

3.2.6 Timing Generator

The timing generator provides the following signals:

a. Red Channel LED ON Time Pulse,

b. Infrared Channel LED ON Time Pulse,

c. Red Channel Sampling Time Pulse,

d. Infrared Channel Sampling Time Pulse, and

e. RSTA Interrupt Generation.

The description that follow is read with the timing diagram in Fig.(3.4).

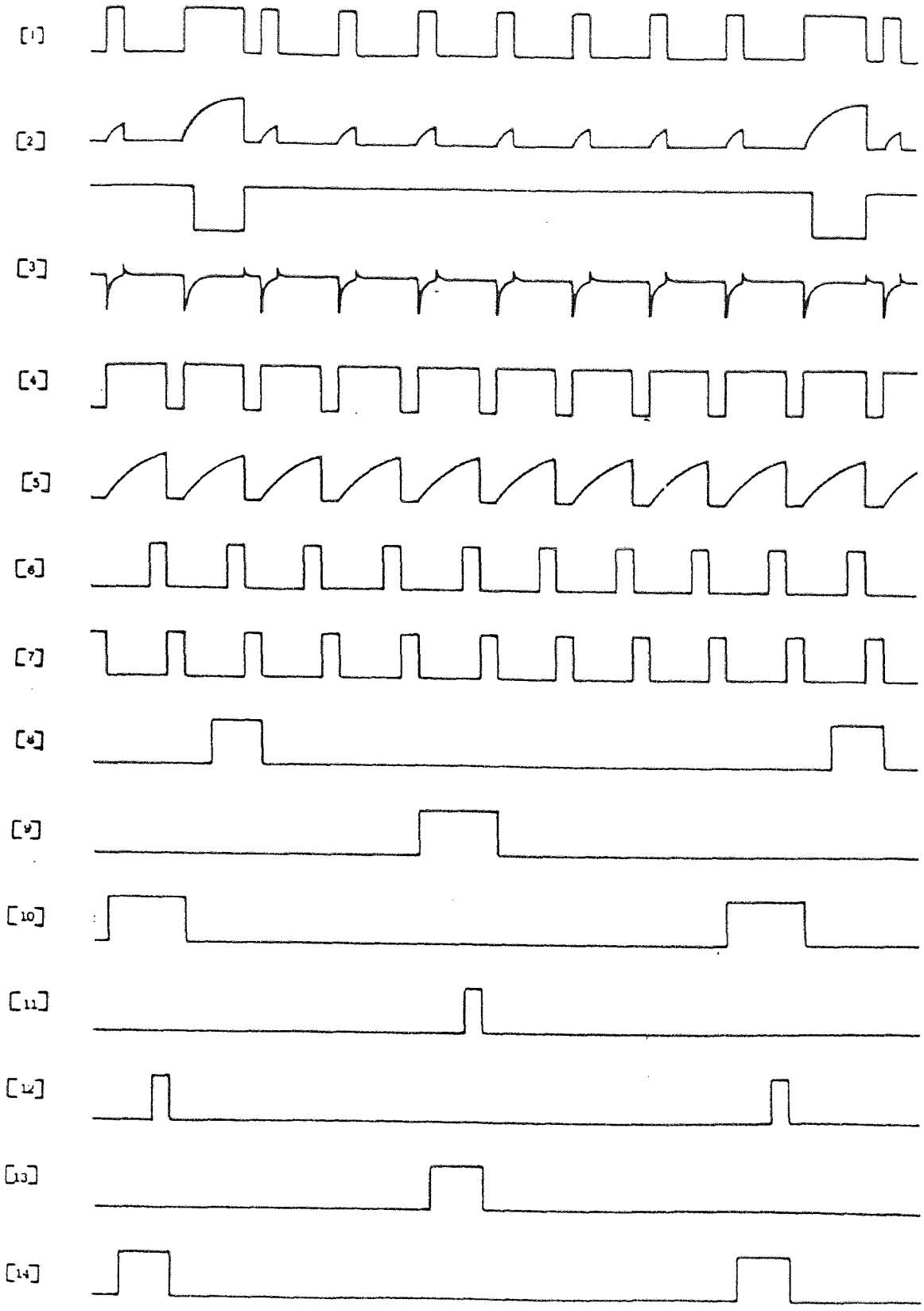

Figure 3.4: Schematic Pulse Sequence from the timing generator

All timing is derived from the timing pulses from the STAT output at IC6/12. The STAT output is inverted at IC7/4 (# 1), which is fed to the pulse width detector consisting of R9, C20 and D4. The output from the pulse detector (# 2) brings the output at IC7/6 to switch negative only when the input IC1/5 is raised above the input threshold. The time constant selected by C20 and R9 allows the 72 μs pulse. This triggers the IC7/6.

The STAT output is also fed to the circuit containing C21, D5 and R12. This circuit differentiates the negative going edge of the STAT (# 3). This is used to trigger IC9/2. IC9 is setup as monostable with a pulse width determined by C22 and R13. The output of IC15/3 a positive going pulse (# 4). The output # 4 is fed to IC10/11 through the delay circuit R14, C23 and D6 to give # 5. IC6/10 triggers only when input is above threshold. This delays the leading edge of the pulse. The output is # 6 at IC10/8.

The output at IC9/3 is inverted at IC10/6 and fed to IC14/5 (# 7). The IC5 is arranged as a latch. Other latch input, IC8/1 is fed from IC7/6. The latch output IC8/3 is fed into a 8 bit shift register IC11, that is clocked by inverted STAT output (# 1). The output of IC 11 pins 5 and 12 are shown in waveform # 9 and # 10.

The output Red Channel LED on time appears at IC9/8 (# 13). It is obtained by ANDing # 4 and # 9.

The output Infrared Channel LED on time appears at IC9/11 (# 14). It is obtained by ANDing # 4 and # 10.

The output Red Channel Sample Time appears at IC9/6 (# 11). It is obtained by Anding # 6 and # 9.

The output Infrared Channel Sample Time appears at IC19/3 (# 12). It is obtained by ANDing # 6 and # 10.

3.2.7 Signal Retrieval

The pulses at IC19/14 whose height is modulated by the amount of blood between the LED and photodiode of the sensor head are fed to the analog switches IC21/1 and IC21/4 which multiplex the red and infrared channels. The analog switches are controlled by the timing generator. The timing generator sets IC21 pins 1 and 2 into a low impedance state only when the RED channel LED pulse is present at IC19/14. The timing generator sets IC29 pins 3 and 4 into a low impedance state only when the Infrared channel LED pulse is present at IC19/14.

The signal retrieval and conditioning of red and infrared pulses is identical. The red channel is explained below. The corresponding infrared devices are shown in brackets[ ].

The output of the analog switch IC21/2 [IC21/3] feeds a holding capacitor C27 [C31] and the buffer IC27/1 [IC27/7]. When the analog switch is set to a low impedance C27 [C31] will charge to the pulse height. This charge is maintained until the next pulse causes the capacitor to charge to the new pulse height value. The output of IC27/1 [IC27/7] is a waveform of the Red [Infrared] channel pulse amplitude. The output IC27/1 [IC27/7] is level shifted by IC28/1 [IC28/7] which is fed to Analog to Digital Converter IC6/8 [IC6/7]. ADC operates in a bipolar mode. Before sending the signal to the ADC at IC6/8 [IC6/7] the signal is passed through a low pass filter. The filter avoids the signal of any high frequency noise.

3.3 Data Acquisition and Microprocessor Control

The two LEDs are sequentially excited with a 36 μS pulse. The reflectances are synchronously sampled and held after amplification. The sampled analog signals are then converted to digital form using an A/D converter (AD7581) on the sensor board assembly. 10 data points are averaged for improving the signal-to-noise ratio. The analysis is done by the microprocessor K-8073.

The analog to digital conversion is performed by IC6, AD7581. This is an 8 channel 8 bit device clocked (at pin 15) by a 1 MHz signal from IC3/11. The device automatically cycles sequentially through each channel. The device takes 80 μS per conversion. So each channel is sampled every 640 μS.

The conversion results can be stored in 8×8 bit RAM on the K-8073 processor. At the end of each conversion STAT (IC6/12) outputs an 8 μS negative pulse. This pulse is extended to 72 μS at the end of each channel-1 conversion. The channel is read from the device by an I/O read cycle that sets the address lines.

The reference is provided for the converter by -2.5Vref. The bipolar offset (BOFS) is used to offset the converter to digitize bipolar signals. The offset voltage and the ADC input signals are under software control of K-8073 processor.

The other devices, such as the electromechanical valve, the sampler and the sensor movement on the cell chamber are controlled by the electromechanical relays which are controlled by the digital output from the microprocessor control board. The timing of sampler rotation and valve opening is decided previously with the help of statistical data of the blood separator and is stored in the memory of the CPU.

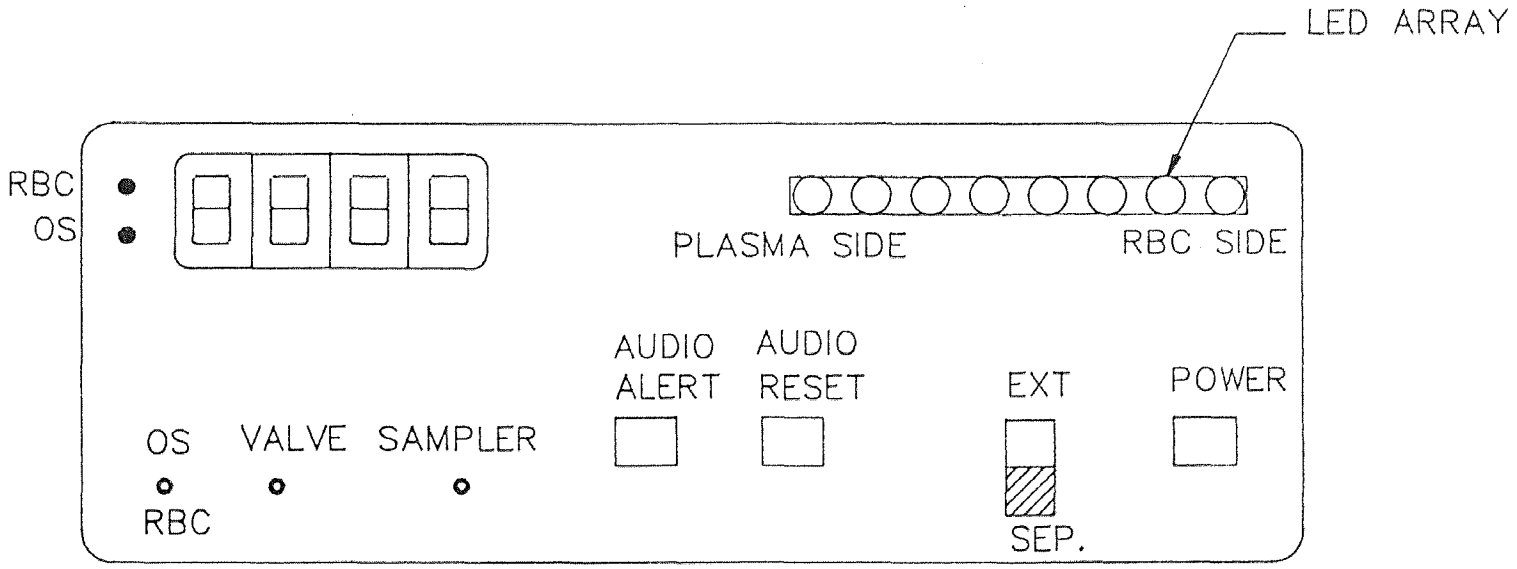

Figure 3.5: Front Panel Diagram of the System

When RSTC Interrupt is generated these data are read from the memory for these controls which activates the corresponding relays.

3.4 Front Panel Controls of the System

The proposed front panel diagram is shown in Fig.(3.5).

The digital display indicates the content of RBCs and Oxygen saturation in the separating blood, which can be selected with the help of the switch. The flashing LED array indicates the position of the sensor on the rotating blood chamber. Here 8 LEDs are utilized. This provision is made for the other types of blood chambers, to adjust the 5 LEDs for sensing.The timing generator used for sensor head controls this array which is similar to sensor array. The distance between two LEDs is same as on the sensor.

Audio Alert is activated when the content of RBCs goes below 10%, which also indicates the opening of the electromechanical valve for collection of blood samples. When the valve opens VALVE indicator lights and remains ON until the valve is closed. The SAMPLER indicator indicates the rotation of the sampler. When the samples are being collected indicator is ON.

One extra control EXT/SEP is proposed for external and online separation measurement.

Chapter 4

Application and Performance

4.1 Theory

According to the fundamental principle of separation of blood components, at hematocrits above 4% RBCs get pushed towards the outer diameter and displaced plasma along with some minerals move closer to the axis of the machine. After a certain duration of time, a distinct separation line is observed in the chamber between the packed red cells and yellow colored plasma. The WBCs form a buffy thin coat between the RBCs and the plasma medium.

The separation front is the interface between the plasma phase and cell phase. Static mode defines the duration of the batch process. The distance of this front from the inner side of the chamber increases in the static mode. As the time passes in the static mode, the separation front gradually moves towards the outer diameter of the chamber, until it reaches a specific position, after which it does not move. This phenomenon can be explained in the following manner.

Initially, RBCs stack as rouleaux and move towards the outer side of the chamber

and they collide with each other and clash against the chamber wall. The sedimentation velocity increases as rouleaux formation takes place along with the settling mechanism. When the RBCs have almost settled in their respective positions, they get packed together and cannot move any further. From that time the separation front does not seem to move any further beyond that particular line of packed cells.

4.2 Centrifuge with Antitwister Mechanism

The centrifuge used for this purpose of blood cell separation was first developed by Ito and Kolbow at NIH. A new machine was constructed by Dr. Sofer's group at the University of Okalahoma and brought to NJIT in 1986. The trapezoidal chamber head was designed by Sofer and Camp of this laboratory. This design is based on Boycott's principle of tapering (slanting) edges. The centrifuge speed can be varied from 300 to 2000 rpm. For our experiments we maintain the speed constant at 600 rpm. The essential attributes of the blood fractionator include a dynamic bearing balance system to reduce vibrations. Tygon tubing for the entry and exit of blood to and from the chamber, a peristaltic pump for control of the blood process stream and an antitwister mechanism to connect the tube directly to the rotating centrifuge rotor in order to prevent any twisting or shearing of the tube and damage to the cells are utilized.

The antitwister cell separator is explained in detail in Appendix A.

4.3 Experimental Procedure

The objective of the experimental work is to utilize the sensor unit for continuous measurement and display of OS and RBC content in the separating blood and overall control of the blood cell separation process.

Here the experimental techniques and features of the blood cell separator are explained. The cell separator with antitwister mechanism is used for blood cell separation which causes less damage to the cells. In this technique, no density gradient chemicals or chemical sedimentation agents are used. The experiments have been performed in a seal-less centrifuge using a trapezoidal chamber head.

The critical parameters for a good separation are hematocrit (HCT), centrifuge speed, withdrawal rate and residence time of blood in the cell chamber.

Bovine blood has been used for the experimental analysis because of two reasons - cow blood is less hazardous to work with than human blood and it is easily available.

Blood was stored at a low, constant temperature in the refrigerator. Before feeding it in the chamber it was stirred properly. Initially, blood was strained through cheese cloth which was slightly soaked in anticoagulant diluent (ACD) solution to remove external impurities. The blood chamber and the connecting tubes were rinsed with ACD solution two or three times before the run. A constant volume of blood (21 ml) was fed through the tube which enters the chamber at its midpoint. The initial parameters, which remained constant throughout the run were defined for the experiment. Centrifuge operating speed was maintained 600 rpm for the runs. The trapezoidal blood chamber was used with the inside thickness of 0.8924 inches. Blood was spun in the chamber and was continuously monitored with the help of the sensor.

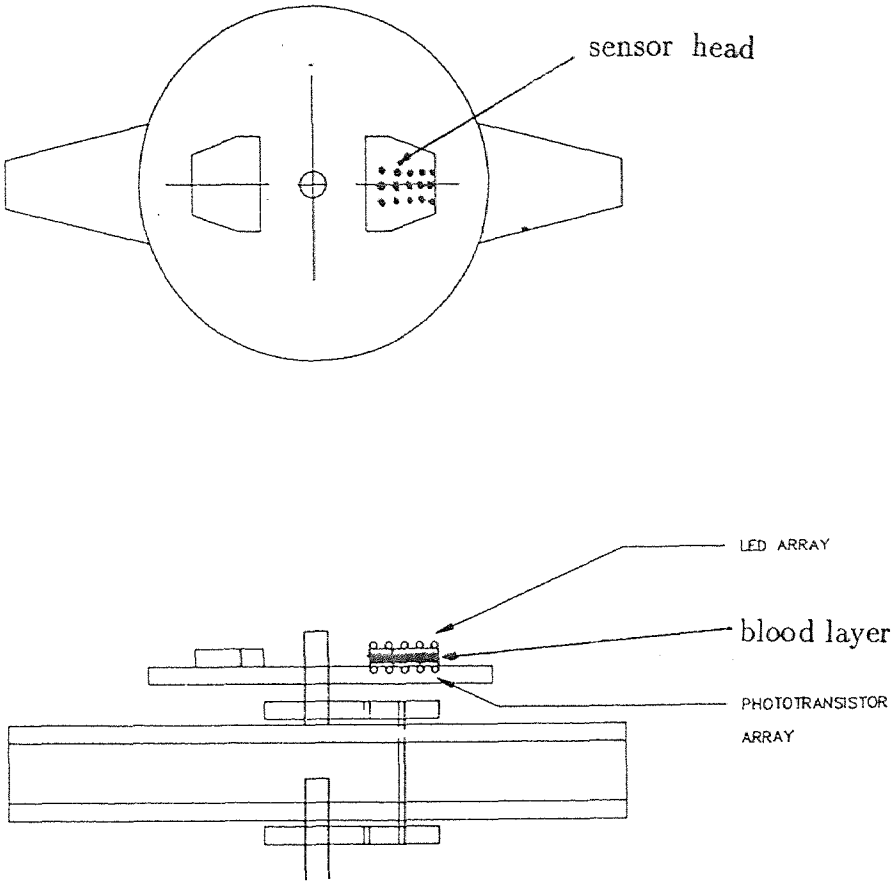

Figure 4.1: Sensor Placement in the Cell Separator

The sensor placement in the cell separator is shown in Fig.(4.1). When the separation front (distinct red layer and yellow plasma layer) becomes prominent the sensor scans around this line. The sensor array of 5 Red and 5 Infrared LEDs are mounted on the blood cell chamber. An array of photodiodes is mounted below the blood chamber.

Tygon tubing is utilized for entry and exit of blood. Through the other tubes which run parallel to the blood tube the wires are passed which are connected to the sensor head from the sensor board. A peristaltic pump for control of blood process stream is used. The speed of the control motor is kept constant. The electromehanical valve and sampler are used to collect the blood samples after the blood cell separation. When the separation is complete the sensor board activates the process of collection of blood samples. The statistical analysis of our previous experiments is utilized to decide the opening time and sampler rotation.

As the overall process of blood separation and sensing is automized, there is no need of analysis for this purpose. The parameters required, RBC content and Oxygen Saturation are displayed in digital form and the samples are collected automatically.

4.4 Calibration

The hemoglobin and RBC content of the separated blood are analyzed by taking the samples and using a Coulter Counter Blood Analyzer model CC-180, TOA Medical Electronics Co. Ltd, Kobe, Japan. The same blood samples are kept in the blood cell chamber. The cell chamber is sealed and is fixed vertically on the stand. The sensor LED arrays are fixed on both sides and the LEDs in front of the blood are used of

sensing. Then the calibration is done on the sensor board to give the same digital output. Since the output is digital, the sensor can be accurately calibrated for any geometry of the blood chamber.

The proposed calibration for OS is theoretical. The experimental and theoretical calibration curves by Takatani *et al* [18] and Schmitt *et al* [5] shown in Fig. (4.2) and Fig. (4.3) respectively are utilized. In the wavelength range λ = 700 nm to 1000 nm the absorption parameters σ_s (eqn [2.4] [2.5]) and scattering parameters are approximately independent of the degree of oxygenation of the hemoglobin contained in the cell. Therefore these curves can be applied for the OS calibration. Though they used infrared wavelengths 795 nm and 820 nm, these curves can be applied since we are using 800 nm and there is no change in absorption and scattering parameters for all three as discussed. The isobestic wavelength is 805 nm.

In fig. (4.2) the reflectances at the two wavelengths versus hemoglobin OS for cow blood are shown for the hematocrit values of 40, 33 and 23 percent. The reflectances at 665 nm decrease nonlinearly as the OS is reduced, while that at 795 nm is a linear function of hemoglobin OS. The reflectance at 795 nm shows a small change (less than 5 percent) over the entire range of hemoglobin OS. With the reduction in the hematocrit, reflectance increases due to overall decrease in the absorption.

Fig. (4.3) is a set of theoretical curves which shows the relationship between the infrared - red diffuse reflectance ratio R820nm/ R660nm and OS as a function of hematocrit. These results indicate that if the ratio were used to estimate OS, significant error would result from hematocrit variations. For blood of normal HCT (42 percent), the error will exceed 1 percent per unit percentage change in HCT for

oxygen saturation values below sixty percent.

Takatani *et al* [18] added a constant C in the numerator as (R795+C)/R665 to minimize the effect of hematocrit variations. As suggested by them we have introduced the constant terms C_1 and C_2 in both the numerator and denominator as $(R660 + C_1)/(R800 + C_2)$ these constants were introduced with the help of the microprocessor for the online measurements.

The value of the constant C varied from 0.020 to 0.090 with increase in RBC size from 25 to 87 cubic microns (from goat to human blood).

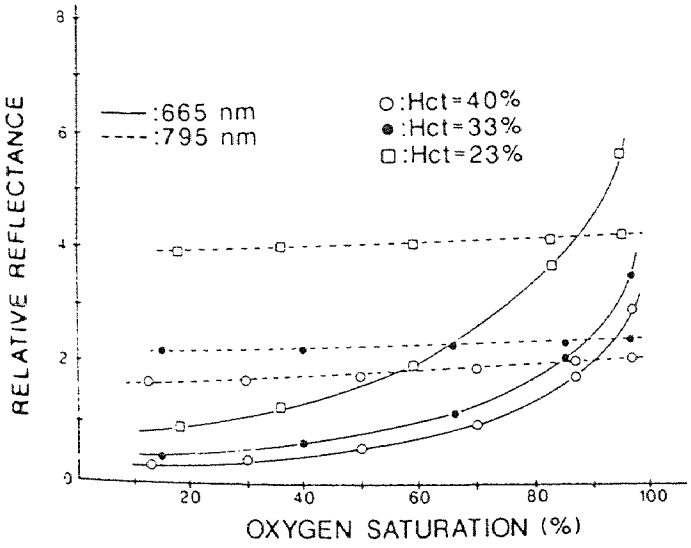

Figure 4.2: Optical reflectances measured at two wavelengths of the prototype optical sensor for hematocrit values of 40, 33, 23 percent. (Source : [18])

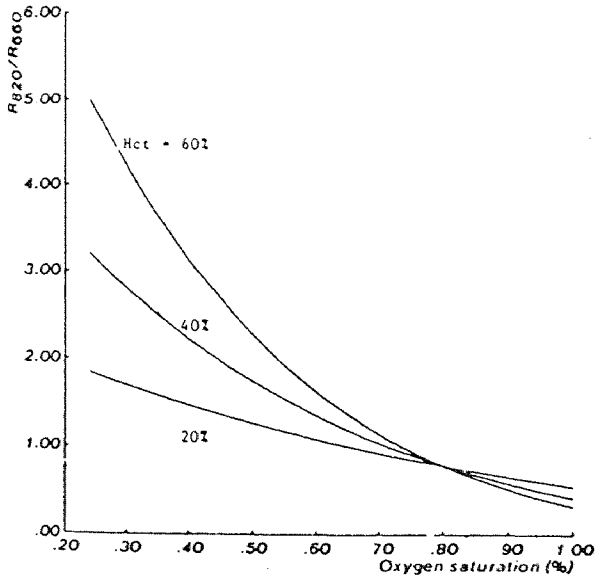

Figure 4.3: Theoretical Curves showing the relationship between the diffuse reflectance ratio R820/ R660 and OS at HCT = 20, 40 and 60 percent. (Source : [5])

Chapter 5

Conclusions

- A theoretical model based on the photon diffusion theory has been developed. This theory has been applied to blood cell separation. It has been shown a useful design tool for sensor development.

- The emission wavelengths 660 nm (visible red) and 800 nm (which is in infrared region is very close to isobestic wavelength of 805 nm for blood) are utilized.

- The effects of hematocrit, sensor separation geometry and blood physiology on the reflection ratio versus hemoglobin OS are reduced by simple addition of the constants C_1 in the numerator and C_2 in the denominator of the ratio term. This method is effective in improving the accuracy of the OS measurement over wide range of hematocrit. This method also minimizes the effect of light scattering.

- With increase in RBC size from 25 to 87 cubic microns (from goat to human blood), the constant value increases from 0.020 to 0.090. [18]

- The sensor system is designed with signal processing electronics and controls for online measurements with the blood cell separation process.

- The feasibility of measuring RBC content and OS with the sensor is demonstrated. The output is in real time and digital form.

- The sensing arrays are mounted on the blood chamber. This avoids the need of fiber optic cable and its associated bending.

- The controls for sampler and valve are designed to collect the blood samples for further blood analysis. Thus the overall operation of the blood separation is controlled.

- The further research in the areas of fiber optic probe design, calibration accuracy and biocompatibility is needed before the sensor can be used for transfusion of blood for patients and vascular application.

- The basic structure of the sensor is flexible enough to allow the measurement of other chemical quantities such as pH, pCO_2. For example, pH can be measured if the red LED is replaced with green LED (λ = 565 nm). Since the absorption spectra of the indicator for sample solutions of varying pH, showed that the peaks of absorption occur at 565 nm and the infrared absorption is independent of that change [14].

- The signal processing electronics can be developed further to view the velocity profiles of the blood components. For this Laser diodes can

be used instead of LEDs using the Laser-induced fluorescence spectroscopy. Then the sensor can be utilized to remove the diseased cells, which has a potential application in treatment of AIDS and cancer. The research is in progress by Dr. Sofer's Research Group at Biotechnology Laboratory, NJIT.

Chapter 6

Appendix A

Antitwister Blood Cell Separator

The centrifuge used for blood cell separation was first developed by Ito and Kolbow at NIH [30]. A new machine was constructed by Dr. Sofer's Group at the University of Okalahoma and brought to NJIT in 1986. The trapezoidal chamber head was designed by Sofer and Camp of this laboratory.

The cell separator utilized is a gear driven device [30][12]. Here the power transmittal is achieved by chain and gear arrangement. Fig.(A.1) shows the schematic representation of the device.

As shown in the figure, the device consists of a rotating head and the antitwister mechanism. The antitwister mechanism consists of two plates stacked vertically as shown. The top plates are separated by aluminium spacers. The distance between the long bottom plate and the lower long plate is maintained by four aluminium spacers of the same length.

The power is supplied by a 1/2 HP ac motor to a stainless steel center shaft. As shaft turns the plate structure also rotates. As the plates turn, power is transmitted to a second solid aluminium shaft.

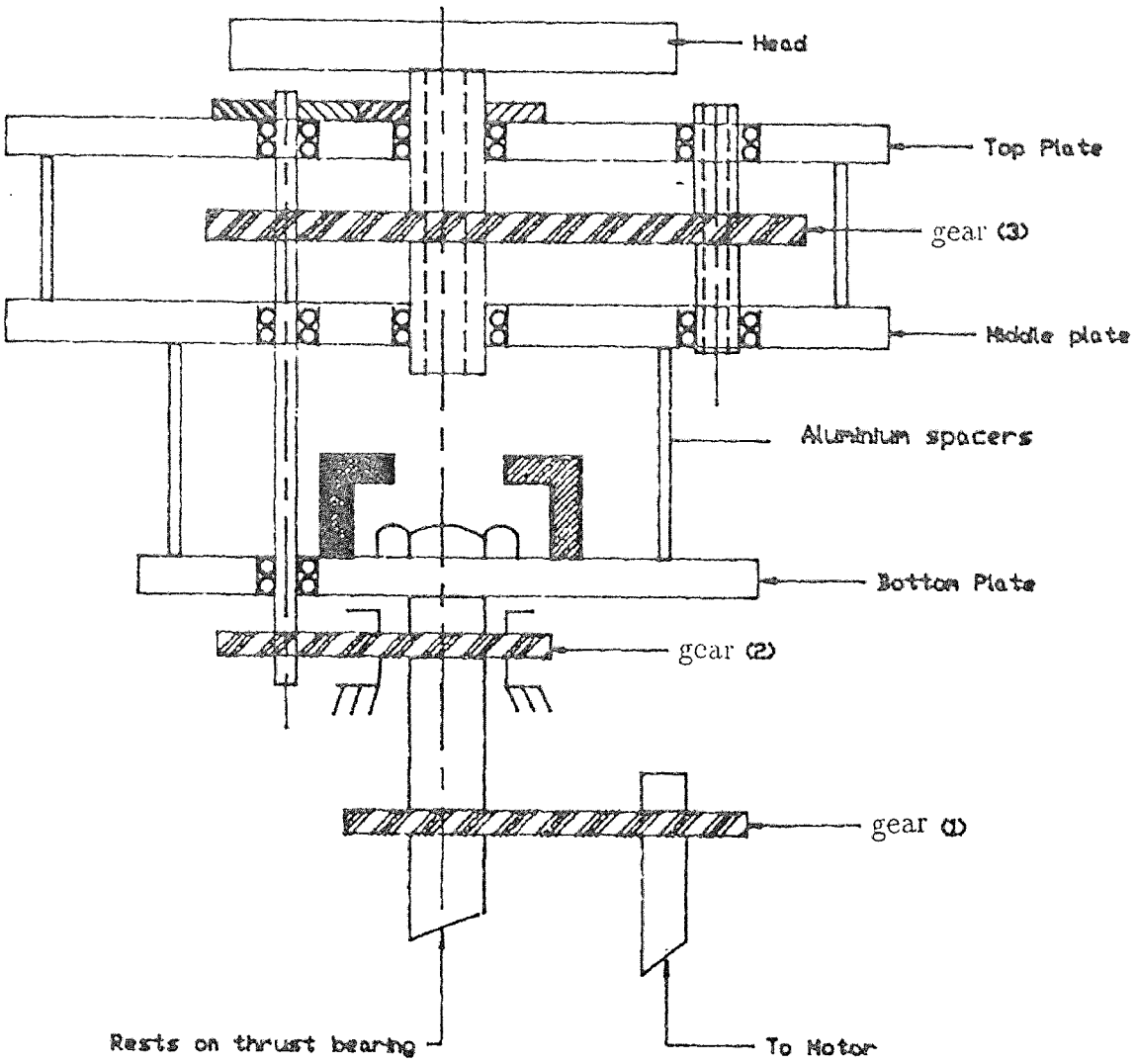

Figure A.1: Schematic of the cell separator with antitwister mechanism (Source : [12])

This shaft rotates at an angular velocity of -w, if the plates are turning at +w. The power transmittal is achieved by the gear and chain arrangement.

The second shaft transmits power to the hollow center shaft that carries head and chamber, through the gears. This rotates head and chamber at an angular velocity of +2w. The second shaft also transmits power to the hollow fourth shaft through gear and chain arrangement. Thus the hollow shaft rotates at an angular velocity of -w.

The Tygon tube containing blood and the blood fraction enters the fourth shaft from the top and is looped into a U shape so that it enters the center shaft from the bottom. Once the tube comes out from the top of the center shaft, it is connected to the chambers mounted on the centrifuge head, in order to prevent any twisting or shearing of the tube and damage to the cells. A peristaltic pump for control of blood stream flow, electromechanical valve and sampler for collection of blood samples are utilized. These are controlled from the sensor board assembly.

The trapezoidal chamber head was designed by Dr. Sofer and Camp of NIH based on Boycott's principle of tapering (slanting)edges. The chamber used is trapezoidal with thickness of 0.8925 inches. The speed of centrifuge is kept constant at 600 rpm for experiments.

The wires are passed through the tubes which are connected to the sensor diode arrays placed on the cell chamber. The shape of the cell chambers used are triangular and trapezoidal. The thickness of all the chambers is kept constant. The sensor head is controlled from the sensor board assembly.

Appendix B

Blood Physiology

Blood is a complex slightly alkaline (pH = 7.4) fluid. It can be divided into about 55 vol% plasma and about 45 vol% living cells suspended in plasma. The hematocrit is defined as the volume percentage of cells and is easily measured by centrifugation of a small blood sample. [29]

The cells consists of about 95% (by number) red blood cells (RBCs) or erythrocytes. White cells comprise another 0.13 % (by number) and the remainder, about 4.9% consists of platelets. The plasma portion of the blood is essentially a dilute (0.15N) electrolyte solution containing about 8 wt% proteins. The RBCs are heavier than plasma. In nonflowing blood the RBCs therefore tend to settle.

B.1 Red Blood Cells

The cells have the shape of a biconcave disc which can deform, into a bullet shaped entity during passage through small capillaries. The mean diameter of a RBC is approximately 8 microns, a thickness of 2 microns at the thickest point and 1 micron or less at the center. The major functions of RBCs are the transport of O_2 and CO_2

throughout the body and buffering the blood so as to regulate pH [29]. Under normal conditions about 60 times as much as O_2 and 20 times more CO_2 can be bound by hemoglobin than can physically dissolve in plasma.

The RBCs, also called as erythrocytes, lack nuclei and organelles. They cannot reproduce. Over a period of time, these cells age and die. Yet the total volume of circulating erythrocytes within the body essentially remains constant. The lost or dead RBCs are replenished by the bone marrow, which is the site of RBC production. The production of RBC by bone marrow fluctuates. In cases of severe erythrocyte destruction, the rate of erythrocyte production increases to keep the total volume of circulating erythrocyte constant.

Erythrocytes are the densest of the three particles found in blood. RBCs settle to the bottom when blood is allowed to stand still, because they have a higher specific gravity than plasma and they tend to aggregate to form rouleax. The settling rate is referred to as sedimentation velocity. When RBCs are affected in certain diseases the sedimentation rate changes, primarily because of the change in the physical characteristics of the sedimentation cells or because of aggregates by clumping and stacking.

Hemoglobin which is present to the extent of more than 33 wt% inside the RBCs consists of four long protein chains to which are bound four 'heme' groups (a ferroprotoporphyrin, a chelating structure composed , in turn, of four pyrrole rings). The globin portion (protein chain) does not bind O_2 or CO_2 but is important as a buffering agent.

B.2 White Blood Cells

White blood cells are also called as leukocytes. WBCs are of several types, but are generally round and somewhat larger than RBCs with diameter of 7 - 20 microns. Lymphocytes, monocytes, eosinophils, neutrophils and basophils are the major WBCs. Although present in much smaller numbers than RBCs, the WBCs are important in combating infections by production of antibodies or by the direct engulfment and digestion of bacteria. The life spans of WBCs (somewhat uncertain) appear to be on the order of a few hours or days.

WBCs provide an immune response for the body. WBCs also originate in bone marrow, but develop further in the lymph tissue and the thymus. Once fully developed, the circulatory system transports them to the places where they are used. The concentration of leukocytes is approximately $7000 cells/mm^3$. There are six different types of leukocytes normally found in blood. These are classified as granular or agranular depending on presence or absence of granules in the cytoplasm.

Polymorphonuclear granulocytes are those which have lobulated nuclei and membrane bound granules. These are further classified as neutrophils and eosinophils. Neutrophils are responsible for phagocytic activity and eosinophils are responsible for allergic reaction.

Monocytes are larger than granulocytes. They themselves may function as phagocytes are may be transformed into macrophages, which is another type of phagocytic cell.

The last type of leukocytes are the lymphocytes. The major type of lymphocytes are B and T. Though both lymphocytes look the same when viewed under the mi-

croscope, functionally these cells are divided into two separate populations. One is responsible for the cellular immunity while the second population is responsible for humoral immunity. The T lymphocytes are those which migrate to and are processed in the thymus glands and are responsible for cellular immunity.

B.3 Platelets

Platelets, small flat cells of about 3 μm diameter, are present in fair numbers and play an important role in the processes of blood coagulation and clotting. Platelets consists of numerous granules. They are colorless and approximately 250 million platelets/ml present in blood. Platelet lives average less than four days.

B.4 Rheological Properties of Blood

Blood is a rather complex fluid, containing a fair number of relatively small molecules and a large variety of macromolecules. Viscosity is defined for a fluid as a ratio of shear stress to shear rate (or velocity gradient).

The viscosity of blood is affected by the magnitude of velocity gradient, temperature, the apparatus used for the viscosity determination, hematocrit variation and the chemical composition of the blood (especially protein content).

Chapter 7

Bibliography

1. R. Brinkman, W. S. Cost, R. K. Koopman and W. G. Zylstra " Continuous Observation on the percentage oxygen saturation of capillary blood in patients," Arch. Chir. Neer., Vol. 1, pp 184-191, 1949.

2. M. L. Polanyi and Hehir," In vivo , Oximeter with fast dynamic response," Rev. Sci.Instrum, vol 33, no.10, pp 1050-1054, 1952.

3. C. C. Johnson, R. D. Palm and D. C. Stewart," A solid state fiber optic oximeter,"J. Ass. Advan. Med. Instrum., vol 5, pp 77-83, 1972.

4. S. Yee, E. Schibi, and V. Krishnan, "A proposed miniature red/ infrared oxymeter suitable for mounting on a catheter tip," IEEE Trans. Biomed. Engg., vol BME-24, pp 195-197, Feb 1986.

5. J. N. Schmitt, J.D. Meindl, and R. G. Mihm," An integrated circuit based optical sensor for in vivo measurement of blood oxygenation.,"IEEE Trans. Biomed. Engg., vol BME-33, pp 98-107, Feb 1986.

6. R. N. Pittman and B. R. Duling, "A new method for measurement of percentage oxyhemoglobin," J. Appl. Phisiol., vol 38, no. 2, pp 315-320, 1975.

7. A. Ishimuru,“ Theory and application of wave propagation and scattering in random media,” *Proc. IEEE,* vol 65, no.7, pp 1030-1061, 1977.

8. D. W. Lubbers, “ Spectrophotometric examinations of tissue oxygenation ,” Oxygen Transport Tissue, Bicher, Ed. pp 45-54, 1975.

9. C. C. Johnson, “Optical diffusion in blood,” IEEE Trans. Biomed. Eng., vol.BME-17, pp 129-133, 1970.

10. S. Takatani and M.D. Graham, “ Theoretical analysis of diffuse reflectance from a two layer tissue model,” IEEE Trans. Biomed. Eng., vol. BME-26, no. 12, pp 656-664, 1979.

11. L. O. Reynolds, “ Three dimensional reflection and transmission equations for optical diffusion in blood,” M. S. Thesis, Univ. Washington, Seattle, WA 1970.

12 Ajit Dastane,“Design of a gear driven antitwister mechanism for a seal-less blood processor, M. S. Thesis, New Jersey Institute of technology, Newark, NJ 1988

13. The Optoelectronics Data book for Design Engineers, Second Edition, Texas Instruments, Inc.

14. K. T. V. Grattan, Z. Mouaziz and A. W. Palmer,“ Dual wavelength optical fiber sensor for pH measurement,” Biosensors 3, pp 17-25, 1987/88

15. K. Kramer, J.O. Elam, G. A. Saxton and W. N. Elam Jr.,“Influence of oxygen

7.1 Experimental Data

For Typical Blood cell Separation : • Machine used for cell separation : VAMPIRE-II.

• Speed of cell separator : 600 rpm.

• Total blood volume : 21 ml.

• No. of blood samples : 8

• Peristaltic pump speed : 200 rpm.

• Tube for entry and exit of blood : Inside diameter = 4mm.

• Sampler collection and valve opening times (in seconds):

I	265.5	136	110	60	40	32	76	65.4	58	48	10
II	202	112	100	70	40	20	65	60	0	47.6	4.5
Specified	250	125	105	65	40	25	70	62	55	48	7

• Blood chambers available :

a)Triangular

b)Trapezoidal

c)Hexagonal

d)Test tube chamber

Blood chamber selected : Trapezoidal with

Inside blood layer thckness = Rx = 0.8925 inches and

Outside thickness = 1.1825 inches

• Sensor Geometry :

No. of sensing LEDs : 5

Sensing distance : 5 cm.

LED and photodiode diameter : 0.200 inches.

Sensor separation distance : more than 3 mm.